Cell. Mol. Life Sci. (2014) 71:4881–4894
DOI 10.1007/s00018-014-1654-8

Cellular and Molecular Life Sciences

RESEARCH ARTICLE

Cyclin A2, a novel regulator of EMT

Nawal Bendris · Caroline T. Cheung · Hon Sing Leong · John D. Lewis · Ann F. Chambers · Jean Marie Blanchard · Bénédicte Lemmers

Received: 29 November 2013 / Revised: 16 May 2014 / Accepted: 19 May 2014 / Published online: 31 May 2014

Abstract Our previous work showed that Cyclin A2 deficiency promotes cell invasion in fibroblasts. Given that the majority of cancers emerge from epithelia, we explored novel functions for Cyclin A2 by depleting it in normal mammary epithelial cells. This caused an epithelial to mesenchymal transition (EMT) associated with loss of cell-to-cell contacts, decreased E-Cadherin expression and increased invasive properties characterized by a reciprocal regulation of RhoA and RhoC activities, where RhoA-decreased activity drove cell invasiveness and E-Cadherin delocalization, and RhoC-increased activity only supported cell motility. Phenotypes induced by Cyclin A2 deficiency were exacerbated upon oncogenic activated-Ras expression, which led to an increased expression of EMT-related transcriptional factors. Moreover, Cyclin A2-depleted cells exhibited stem cell-like properties and increased invasion in an in vivo avian embryo model. Our work supports a model where Cyclin A2 downregulation facilitates cancer cell EMT and metastatic dissemination.

Keywords Aggressiveness · Cyclin A · Invasiveness · Stemness

Abbreviations

CycA2	Cyclin A2
EMT	Epithelial to mesenchymal transition
NMuMG	Normal murine mammary gland
TGFβ	Transforming growth factor β

Introduction

Cyclin A2 expression in human cancer is usually linked to cell proliferation. However, in renal, colorectal and prostate carcinomas [1, 15, 25, 29], tumors with low levels of Cyclin A2 were shown to be more aggressive than those with high Cyclin A2 expression. Similarly, there is an inverse correlation between Cyclin A2 levels and invasiveness of oral squamous cell carcinoma (OSCC) both in vitro and in vivo [46]. In addition, we recently found decreased expression of Cyclin A2 in metastases relative to primary tumors in colorectal cancer [4].

There is a precedent for cell cycle regulators to have new functions that may influence tumorigenesis [7, 9]. Here, we explore these novel Cyclin A2 functions in an epithelial context, in particular its role in the epithelial to mesenchymal transition (EMT).

EMT plays a role during early embryonic development and is reactivated during adult tissue regeneration and wound

Electronic supplementary material The online version of this article (doi:10.1007/s00018-014-1654-8) contains supplementary material, which is available to authorized users.

N. Bendris · C. T. Cheung · J. M. Blanchard · B. Lemmers (✉)
Institut de Génétique Moléculaire de Montpellier, CNRS, 1919 route de Mende, 34293 Montpellier, France
e-mail: benedicte.lemmers@igmm.cnrs.fr
e-mail: jean-marie.blanchard@igmm.cnrs.fr

N. Bendris · C. T. Cheung · J. M. Blanchard · B. Lemmers
Université Montpellier 2, Place Eugène Bataillon, 34095 Montpellier, France

N. Bendris · C. T. Cheung · J. M. Blanchard · B. Lemmers
Université Montpellier 1, 5 Bd Henry IV, 34967 Montpellier, France

N. Bendris
Department of Cell Biology, UT Southwestern Medical Center, 5323 Harry Hines Blvd, Dallas, TX 75235, USA

H. S. Leong · J. D. Lewis · A. F. Chambers
Translational Prostate Cancer Research Group, London Regional Cancer Program, London, ON, Canada

repair [41]. Moreover, clinical evidence suggests that upregulation of EMT inducers in cancer cells correlates with tumor aggressiveness, metastasis and poor patient prognosis [11, 35, 48]. EMT is triggered by a network of signals emanating from the tumor stroma [26, 49]. Notably, Ras and TGFβ have been shown to cooperate in promoting EMT, whereby the activating Val12 mutation of Ras potentiates this process [22].

EMT is characterized by loss of E-Cadherin from the plasma membrane and acquisition of mesenchymal markers [42]. The expression of multiple transcription factors, in particular the E2A gene products E12 and E47, members of the Snail and Twist families, Zeb1 and Zeb2 [5, 39, 47] are also induced. Moreover, cells undergoing EMT acquire invasive capabilities following increased expression or activation of RhoGTPases, such as Rac1, Cdc42 and RhoC [27]. In addition, cells can acquire stem cell markers, which identify them as potential tumor-initiating cells responsible for further spreading in vivo [17].

Here, we explore the effect of Cyclin A2 inactivation in the EMT process. Depletion of Cyclin A2 in the mouse mammary gland epithelial cell line NMuMG conferred a spindle-like morphology to the cells and a loss of cell–cell contacts, along with both decreased expression of E-Cadherin and its delocalization from the membrane. Cyclin A2-depleted NMuMG cells showed increased 3D invasive properties, which correlated with decreased RhoA and increased RhoC activities. This mesenchymal phenotype was enhanced by transformation with H-RasV12, as evidenced by upregulation of associated transcription factors and metalloproteases. Knockdown of RhoA potentiated cell invasion and disrupted E-Cadherin localization to the plasma membrane, whereas our data identify RhoC as a major regulator of cell invasion in the Cyclin A2-depleted cells. Sh CycA2 transformed cells showed increased formation of tumorospheres and expression of stem cell markers, suggesting that loss of Cyclin A2 may promote cancer stem cell capabilities. Moreover, the in vitro effects of Cyclin A2 depletion were corroborated by in vivo experiments showing an enhanced invasion of Cyclin A2 knockdown cells in an avian embryo model.

Overall, our study establishes Cyclin A2 as a novel regulator of metastasis through modulation of EMT, which sheds new light on why low Cyclin A2 expression is associated with poor prognosis in some cancers.

Materials and methods

Plasmids and siRNA

shRNA a and b were both used for experiments:

a: 5′-GAAATGGAGGTTAAATGA-3′
b: 5′-GTAGCAGAGTTTGTGTATA-3′.

They were cloned into RNAi-Ready pSIREN-RetroQ vector (Clontech, Mountain View, CA).

A plasmid containing mouse wild-type RhoC fused to EGFP was a kind gift from J.C. Der (University of North Carolina, Chapel Hill, USA). siRNA directed against mouse RhoA and RhoC were purchased from Thermo Scientific (Waltham, MA) as smartpools. They were transfected using Lipofectamine 2000 (Invitrogen, Carlsbad, CA) at 10 nM concentration. Assays (immunfluorescence, Western blot analysis, invasion assay) were performed 48–72 h following transfection.

Quantitative real time PCR (qRT-PCR)

RNA was purified using RNeasy kit (Qiagen, Hilden, Germany). Reverse transcription was performed using Superscript III (Invitrogen) according to standard protocols. qRT-PCR was performed using SYBR Green (Roche, Basel, Switzerland) with the primers listed in Supplementary Table 1. Briefly, cDNA samples were diluted and subjected to 40 cycles of PCR at 95 °C for 10 s, 60 °C for 15 s and 72 °C for 15 s. Internal controls used were GUS (beta-glucuronidase), HPRT (hypoxanthine guanine phosphoribosyl transferase 1) and TBP (TFIID TATA box binding protein). Reactions were performed on a LightCycler 480 (Roche) machine.

qPCR primer sequences

Gene name	Forward/ reverse	Sequence 5′–3′
E12	Forward	GGGAGGAGAAAGAGGATGA
	Reverse	GCTCCGCCTTCTGCTCTG
E47	Forward	GGGAGGAGAAAGAGGATGA
	Reverse	CCGGTCCCTCAGGTCCTTC
E-Cadherin	Forward	CTGCTGCTCCTACTGTTTC
	Reverse	CTGGCTCAAATCAAAGTCC
Fibronectin	Forward	GCGACTCTGACTGGCCTTAC
	Reverse	CCGTGTAAGGGTCAAAGCAT
GUS	Forward	GATTCAGATATCCGAGGGAAAGG
	Reverse	GCCAACGGAGCAGGTTGA
HPRT	Forward	GCAGTACAGCCCCAAAATGG
	Reverse	GGTCCTTTTCACCAGCAAGCT
MMP-3	Forward	GGAAATCAGTTCTGGGCTATACGA
	Reverse	TAGAAATGGCAGCATCGATCTTC
MMP-14	Forward	GGAGACGGAGGTGATCATCATTG
	Reverse	GCGTCCCATGGCGTCTGAAGA
N-Cadherin	Forward	GGCAGAAGAGAGACTGGGTC
	Reverse	GAGGCTGGTCAGCTCCTGGC
Nanog	Forward	TCTTCCTGGTCCCCACAGTTT
	Reverse	GCAAGAATAGTTCTCGGGATGAA
Oct4	Forward	AGAGGATCACCTTGGGGTACA
	Reverse	CGAAGCGACAGATGGTGGTC

Gene name	Forward/ reverse	Sequence 5′–3′
Slug	Forward	CCATGCCATCGAAGCTGAG
	Reverse	GGCCAGCCCAGAGAACGTA
Sip1/Zeb2	Forward	TAGCCGGTCCAGAAGAAATG
	Reverse	GGCCATCTCTTTCCTCCAGT
Six1	Forward	GAATCAACTCTCTCCTCTGG
	Reverse	TTAGGAACCCAAGTCCACCA
Snail	Forward	CACTGCCACAGGCCGTATC
	Reverse	CTTGCCGCACACCTTACAG
TBP	Forward	ACTTCGTGCAAGAAATGCTGAAT
	Reverse	CAGTTGTCCGTGGCTCTCTTATT
Twist 2	Forward	GCAAGAAATCGAGCGAAGAT
	Reverse	GCTCTGCAGCTCCTCGAA
Zeb1	Forward	GCTGGCAAGACAACGTGAAAG
	Reverse	GCCTCAGGATAAATGACGGC

Cell culture, transfections and infections

NMuMG and NMuMGRasV12 cells were maintained in DMEM with 10 % fetal calf serum (FCS) supplemented with insulin (10 μg/ml). They were purchased from ATCC (CRL-1636, Manassas, VA). Transfections were performed using Lipofectamine 2000 (Invitrogen). For virus infection, cells were selected for at least 2 days in the presence of 2μg/ml puromycin (Invitrogen) or 100 μg/ml hygromycin. For rescue experiments, cells previously infected with sh-a directed against Cyclin A2 were infected with a retrovirus coding for Wt Cyclin A2 resistant for sh-a. Infections with control virus are denominated as PMSCV (plasmid derived from the Murine Stem Cell Virus).

FACS analysis of cell cycle and cell viability

Following 12 h of culture in non-adherent conditions, tumorospheres were trypsinized and cells (10^6) incubated with 7AAD (1 μg/ml in PBS) to evaluate cell death. 7AAD staining was measured by FACS analysis on a FACSCalibur (BD Biosciences, San Jose, CA). For cell cycle analysis, 10^6 cells were fixed overnight using 90 % ethanol. Cells were spun, washed once with PBS and resuspended in 500 μl of PBS-7AAD (1 μg/ml)-RNase(200 μg/ml) for 30 min before being analyzed.

Kinase assay

Cells were lysed in the following buffer : 50 mM Tris pH 7.5, 250 mM NaCl, 0.1 % Triton X100, 5 mM EDTA, 1 mM DTT, 50 mM NaF, 0.1 mM Na_3VO_4. 500 μg of proteins were immunoprecipitated using either an anti-CDK2 (sc-163, Santa Cruz Biotechnologies, Santa Cruz, CA) or and anti-CDK1 (sc-54, Santa Cruz) for at least 3 h at 4 °C. Immunoprecipitates were washed three times in lysis buffer and divided in two. One half was washed once in kinase buffer (10 mM Tris pH 7.5, 10 mM MgCl2, 1 mM DTT, 100 μM ATP) and the other half was resuspended for Western blot analysis. The kinase reaction was performed as follows: 20 μl of kinase buffer containing 0.2 μCi of ^{33} P-γATP and 5 μg of Histone H1 were added in each immunoprecipitate. The reaction was incubated at 37 °C for 30 min then stopped by the addition of 1 μl of 0.5 M EDTA. The entire reaction was transferred onto a Whatman Grade *P81* paper, which was washed three times in 0.75 % phosphoric acid solution, then in 95 % ethanol and dried. Samples were transferred in scintillation buffer and counted using the Tri-Card 2900 TR analyzer from Packard. Western blot analysis was performed in parallel to check total and immunoprecipitated CDK1 and CDK2 protein levels which were similar between both sh Luc and sh CycA2 cells.

Antibodies, immunofluorescence and immunoprecipitation

Antibodies used for immunoblotting included: anti-CyclinA2 (clone CY-A1—Sigma-Aldrich, St. Louis, MO; and sc-751, Santa Cruz Biotechnology), anti-RhoA (sc-418, Santa Cruz Biotechnology), anti-RhoC (D40E4, Cell Signaling, Danvers, MA), anti-Rac1 (clone 102, BD Transduction Laboratory, Franklin Lakes, NJ), anti-E-Cadherin (clone36, BD Transduction Laboratory), anti-non phosphorylated active β Catenin (Cell Signaling) and anti-GAPDH (G9545, Sigma). Secondary HRP-conjugated antibodies were obtained from Pierce Biotechnology (Thermo Scientific, Rockford, IL).

Antibodies used for immunofluorescence staining were: anti-Vinculin, (clone hVIN, Sigma), anti-E-Cadherin (clone36, BD Transduction Laboratory), anti-p120 Catenin (clone98, BD Transduction Laboratory), anti-β Catenin (clone 6B3, Cell Signaling), and anti-Vimentin (3932, Cell Signaling). Staining of F-Actin was performed using Phalloidin conjugated with Rhodamine (Sigma). Secondary antibodies were AlexaFluor conjugates (Invitrogen).

Prior to immunofluorescence analysis, cells were fixed with 3.2 % paraformaldehyde and permeabilized with 0.2 % Triton-X-100 for Phalloidin staining. For p120 Catenin, cells were treated for 10 min at −20 °C in methanol/acetone (1:1), and for β Catenin/E-Cadherin stainings, cells were fixed 30 min in 100 % ethanol (−20 °C) then a few seconds in acetone [13]. Fixed cells were viewed using Axioimager Z1 (Carl Zeiss, Inc., Oberkochen, Germany) with 63X Plan-Apochromat 1.4 oil lens (Carl Zeiss, Inc.). Images were collected using a CoolSnap HD2 CCD camera (Roper Industries, Sarasota, FL) driven by MetaMorph 7.1 Software.

Immunoprecipitations were performed using GFP-Trap® beads (Chromotek, Planegg-Martinsried, Germany) in

NP40 lysis buffer according to manufacturer instruction for 2 h at 4 °C. After washes, beads were resuspended in Laemmli buffer for Western blot analysis.

Pull-down of active Rho GTPases

Cells were lysed and incubated for 1 h at 4 °C, either with 60μg Rhotekin-RBD protein GST beads or 20μg PAK-GST protein beads (Cytoskeleton, Denver, CO) for RhoA and RhoC or Rac1 pull-down, respectively [4, 10]. Following SDS-PAGE and Western blot analysis using anti-RhoA, anti-RhoC and anti-Rac1 antibodies, GTPase activation was evaluated by measuring band intensities with ImageJ software. The activation index was calculated as pull-down/input/GAPDH intensity ratio.

Invasion assays

Invasion assays were performed in 96-well dishes (PerkinElmer, Waltham, MA) coated with 0.2 % bovine serum albumin (Sigma, A-8806) and bovine collagen (1 mg/ml), as described previously [4, 38]. After 24 h, cells were fixed with paraformaldehyde (4 % final concentration) and stained with 2 μg/ml Hoechst (Molecular Probes, Invitrogen). Confocal Z slices were collected from each well at 0 μm and 50 μm from the bottom. The invasion index was calculated as the ratio of cells at 50/0 μm. Cell invasion was monitored using an Arrayscan VTI Live inverted microscope, and the nuclear staining was quantified with Cellomics software.

Tumorosphere assay

10^6 cells of the different genotypes were plated in low-adhesion plates and cultivated in DMEM without serum for 48 h. After 48 h, tumorospheres were harvested, dissociated with trypsin and cell number was evaluated using a Z1 Coulter counter.

Quantitation of extravasation efficiency rates in chicken embryos and cancer cell extravascular migration in vivo

For the quantification of extravasation, fertilized chicken eggs were incubated in a rotary incubator at 37 °C with 90 % humidity for 4 days before being removed from the shell, placed in covered dishes and then incubated at 37 °C with 90 % humidity until usage [23, 24]. On day 13 of embryonic development, 10^5 cells of the different genotypes were intravenously injected into a vein within the chorioallantoic membrane (CAM, $N = 5$ each group) [23, 24]. Stitched images of the ROI were acquired immediately after injection and at 24 h post-injection on an upright Zeiss Examiner and a Hamamatsu EMCDD camera using Volocity software (PerkinElmer). CAM vasculature was labeled with fluorescent Lens Culinaris Agglutinin (LCA, Vector Laboratories, Burlingame, CA) at 24 h post-injection timepoint, and cells were visualized using a spinning disk confocal microscope (Quorum Technologies, Waterloo, ON, Canada) [3]. Extravascular cells were identified as being present within the underlying stroma, and not within the same *Z*-plane as the CAM lumen [3]. At least 100 cells for each ROI at $t = 0$ were analyzed and enumerated.

For extravascular migration, embryos injected with 10^5 cells at day 9 of development were incubated at 37 °C with 90 % humidity until day 16 of development. Randomly selected micrometastases were imaged intravitally using an upright AxioExaminer microscope (Zeiss) fitted with a temperature-regulated enclosure, laser diode/shutter unit, EMCCD camera, Yokogawa spinning disk console and 10X microscope objective. Three-dimensional image sets of at least 5 regions of interest (ROI) were acquired for each embryo every 15 min during 12–16 h. Volocity (PerkinElmer) was used to generate migration tracks of individual cells within each ROI, in which at least 5 individual migration tracks were analyzed. Each group of embryos (control, Cyclin A2 knockdown) included $n = 4$.

Statistical analysis

Data are reported as arithmetic mean ± SEM. Statistical analyses were carried out using nonparametric Mann–Whitney test or one-way ANOVA and post hoc tests including Dunnett's and Tukey's tests performed with Prism software. Statistical significance was defined as $P \leq 0.05$.

Results

Cyclin A2-depleted epithelial cells adopt a fibroblastic morphology and undergo EMT

We infected normal mouse mammary gland epithelial cells (NMuMG) with expression vectors for small hairpin RNAs that target the Cyclin A2 transcript (sh CycA2) and firefly luciferase (sh Luc) as control. While Cyclin A2 knockdown had no major effect on cell proliferation, the cells showed a slight accumulation in S phase which correlated with decreased CDK2 and CDK1 activities, the latter probably due to a decreased cell proportion in G2 M (online resources 1 and 2a). Moreover, the cells showed a more elongated morphology (Fig. 1 and online resource 2b). This was also true for the bipotential mouse embryonic liver (BMEL) cell line and 67NR, a mouse mammary carcinoma epithelial cell line (online resource 2b). When cultivated in collagen (3D), or as a monolayer, Cyclin A2-depleted cells adopted a tubular shape characteristic of mesenchymal cells, or displayed cytoplasmic protrusions (Fig. 1a and online resource 2b). E-Cadherin

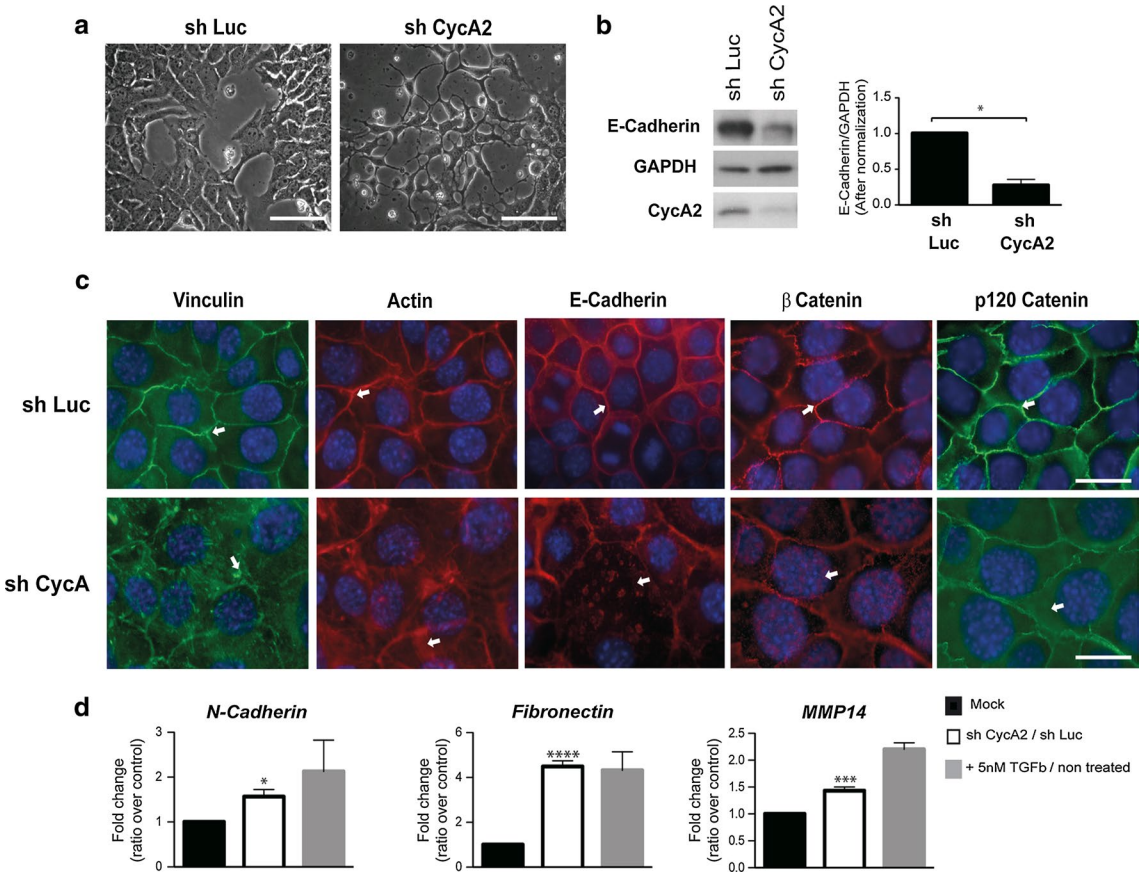

Fig. 1 Induction of mesenchymal traits following Cyclin A2 depletion in NMuMG cells. **a** Visualization of sh Luc and sh CycA2 NMuMG cells by light microscopy. *Scale bar* 200 μm. **b** Western blot analysis of E-Cadherin in Cyclin A2-depleted cells and sh Luc NMuMG cells. E-Cadherin expression was quantified by densitometry and normalized to that of GAPDH ($n = 3$, $^*P = 0.01$). **c** Staining of F-Actin using Phalloidin-Rhodamine, β Catenin (*red*) or Vinculin (*green*), E-Cadherin (*red*) and p120 Catenin (*green*) in sh Luc and sh CycA2 NMuMG cells. *Scale bar* 20μm. **d** qPCR analysis of N-Cadherin, Fibronectin and MMP-14 mRNA levels. The values are expressed as fold change, where sh CycA2 was compared to sh Luc and TGFβ treated cells to untreated cells. Data are represented as mean ± SEM

protein levels decreased, and the remaining protein relocalized from the membrane junctions to the cytoplasm (Fig. 1b, c). This corresponded to diminished contact between cells, and an increase in cell size, as well as the formation of stress fibers and a redistribution of focal adhesions as detected by Phalloidin and Vinculin staining, respectively (Fig. 1c). The membrane-proximal proteins, β Catenin and p120 Catenin, shifted from cell junctions to the nucleus and the cytoplasm, respectively (Fig. 1c). Furthermore, N-Cadherin and Fibronectin mRNA levels (1.6 ± 0.5, $P < 0.01$; 4.5 ± 1.0, $P < 0.0001$, respectively) were consistently increased following the loss of Cyclin A2 relative to controls. Similarly, Cyclin A2 depletion led to a significant upregulation of the mRNA coding for the membrane-associated regulatory metalloproteinase MMP-14 (1.5 ± 0.2, $P < 0.0005$), which has been shown to be expressed by invasive carcinomas undergoing EMT (Fig. 1d). For comparison, NMuMG cells were treated with TGFβ, a known EMT-inducer in these cells.

We performed rescue experiments by infecting sh CycA2 cells using a retrovirus coding for shRNA-resistant Wt CyclinA2 tagged with Flag. In these conditions, E-Cadherin and p120 Catenin translocation from the membrane to the cytosol was clearly reversed (online resource 3a), and cell-to-cell junctions appeared intact like sh Luc cells. Moreover, Western blot analysis of active β catenin showed a clear increase in absence of Cyclin A2 which returned to control levels after Cyclin A2 reexpression (online resource 3b).

Altogether, Cyclin A2 depletion leads to an EMT phenotype.

Cyclin A2 knockdown promotes invasion and has opposite effects on RhoA and RhoC activities

During EMT, cells acquire enhanced invasive capacities. We used a 3D collagen matrix to measure invasion by sh Luc and sh CycA2 NMuMG cells. Consistent with the

results above, Cyclin A2 knockdown increased invasion in NMuMG cells (Fig. 2a), which was reversed following infection of sh CycA2 cells with a retrovirus coding for shRNA-resistant Wt Cyclin A2 (online resource 3c). Rho GTPases control Actin dynamics, membrane protrusion and thereby cell migration [19, 36]. We measured RhoA, RhoC and Rac1 activities in Cyclin A2-depleted NMuMG cells using a GTP-bound GTPase pull-down assay. Cell extracts were incubated with either GST-Pak1-PBD for Rac1 or GST-Rhotekin-RBD for RhoA and RhoC. The bound proteins were visualized by immunoblotting for Rac1, RhoA and RhoC. While Rac1 activation was not affected by Cyclin A2 knockdown (Fig. 2b), a strong decrease in activity of RhoA (Fig. 2c) and an increase in that of RhoC relative to control cells expressing sh Luc (Fig. 2d) were observed.

We previously found an interaction between Cyclin A2 and RhoA [4]. Given the strong sequence conservation between RhoA and RhoC, we investigated whether RhoC could also interact with Cyclin A2. Lysates from cells expressing GFP-tagged RhoC were incubated with tag-specific antibodies, and the bound complexes were analyzed by immunoblotting. Indeed, endogenous Cyclin A2 was found to co-precipitate with RhoC as well (Fig. 2e).

Mesenchymal traits of Cyclin A2-depleted cells are increased upon Ras expression

Activated Ras (H-RasV12) facilitates EMT in several cell lines [40], and Cyclin A2 knockdown in a RasV12-overexpressing background increased the mesenchymal traits of the cells as shown by qPCR analysis of several EMT marker genes (Fig. 3). Indeed, mRNA level for N-Cadherin was significantly increased (2.1 ± 0.19, $P < 0.0001$) to a greater extent than with sh CycA2 alone. Those for E-Cadherin (0.5 ± 0.066, $P < 0.05$) were diminished relative to vehicle control, and NMuMG cells with Cyclin A2 knocked down (Fig. 3a). Consistent with this, there was an associated increase in the mRNA levels of transcription factors involved in E-Cadherin repression, including E12 (2.1 ± 0.23, $P < 0.0001$), E47 (2.3 ± 0.39, $P < 0.0001$), Twist 2 (3.4 ± 0.90, $P < 0.0001$) and Slug (2.0 ± 0.26, $P < 0.0001$ without RasV12 and 3.9 ± 0.52, $P < 0.0001$ in its presence) as compared to both sh CycA2 alone and control cells (Fig. 3b). Further, Sip1/Zeb2 transcript levels were equally upregulated upon CycA2 depletion with or without RasV12 (1.7 ± 0.097, $P < 0.001$; 1.7 ± 0.068, $P < 0.001$; respectively).

We analyzed the transcript levels of the regulatory proteases, MMP-3 and -14 (Fig. 3c), which are important components in EMT. Like Fibronectin, MMP-14 was upregulated by Cyclin A2 deficiency with or without oncogenic Ras (1.5 ± 0.16, $P < 0.0005$; 1.7 ± 0.03, $P < 0.001$). In contrast, while MMP-3 was slightly decreased by sh CycA2 alone (0.3 ± 0.04, $P < 0.001$), enhanced MMP-3 mRNA expression (4.2 ± 0.066, $P < 0.001$) was observed and required both RasV12 and diminished Cyclin A2 levels. Finally, analysis of invasion rate and RhoC activity of Cyclin A2-depleted cells in the context of Ras showed increases in both by comparison to their controls (online resource 4). Thus, while Cyclin A2 deficiency alone can activate hallmarks of EMT, they are increased by expression of activated Ras in conjunction with Cyclin A2 depletion (resource online 5).

RhoA knockdown mimics changes induced by Cyclin A2 deficiency while that of RhoC reverses the effect on cell invasion

Using siRNA, we determined whether RhoA can recapitulate the phenotype induced by diminished Cyclin A2 levels. RhoA knockdown in NMuMGRasV12 cells had increased invasive properties in 3D matrix, and strikingly, these cells showed a fibroblastic morphology together with delocalization of E-Cadherin and p120 Catenin to the cytosol, although E-Cadherin protein levels and transcripts were unchanged (Fig. 4a–c). Moreover, the mRNA levels of the EMT-associated transcription factor E47 (1.4 ± 0.2, $P < 0.001$) and mesenchymal marker Fibronectin (1.8 ± 0.4, $P < 0.001$) were increased in the absence of RhoA, although most of the other EMT markers were not enhanced (Fig. 4d).

To elucidate the involvement of RhoC in the effects mediated by Cyclin A2 depletion, we used siRNA against RhoC in sh CycA2 NMuMGRasV12 cells as an attempt to revert their phenotype. Interestingly, RhoC depletion in these cells greatly impaired cell invasion with a decrease in MMP3 mRNA level (0.5 ± 0.1, $P < 0.0001$), but there was no reversion of the mesenchymal morphology (not shown), and no significant effect on other EMT-associated markers (data not shown).

Overall, RhoA depletion appears to recapitulate some of the phenotypes observed in the absence of Cyclin A2, i.e., increased invasiveness, elongated cell morphology, cell adhesion molecule delocalization and upregulation of some EMT markers. In contrast, RhoC depletion in the absence of Cyclin A2 affects only cell invasion.

CyclinA2 depletion enhances tumorosphere formation and stem cell marker expression

After undergoing EMT, cells display certain stemness characteristics, including the expression of stem cell markers, the ability to form tumorospheres under conditions of low adherence and a high tumorigenic potential [28]. NMuMGRasV12 cells formed tumorospheres under non-adherent conditions. Ablation of Cyclin A2 increased

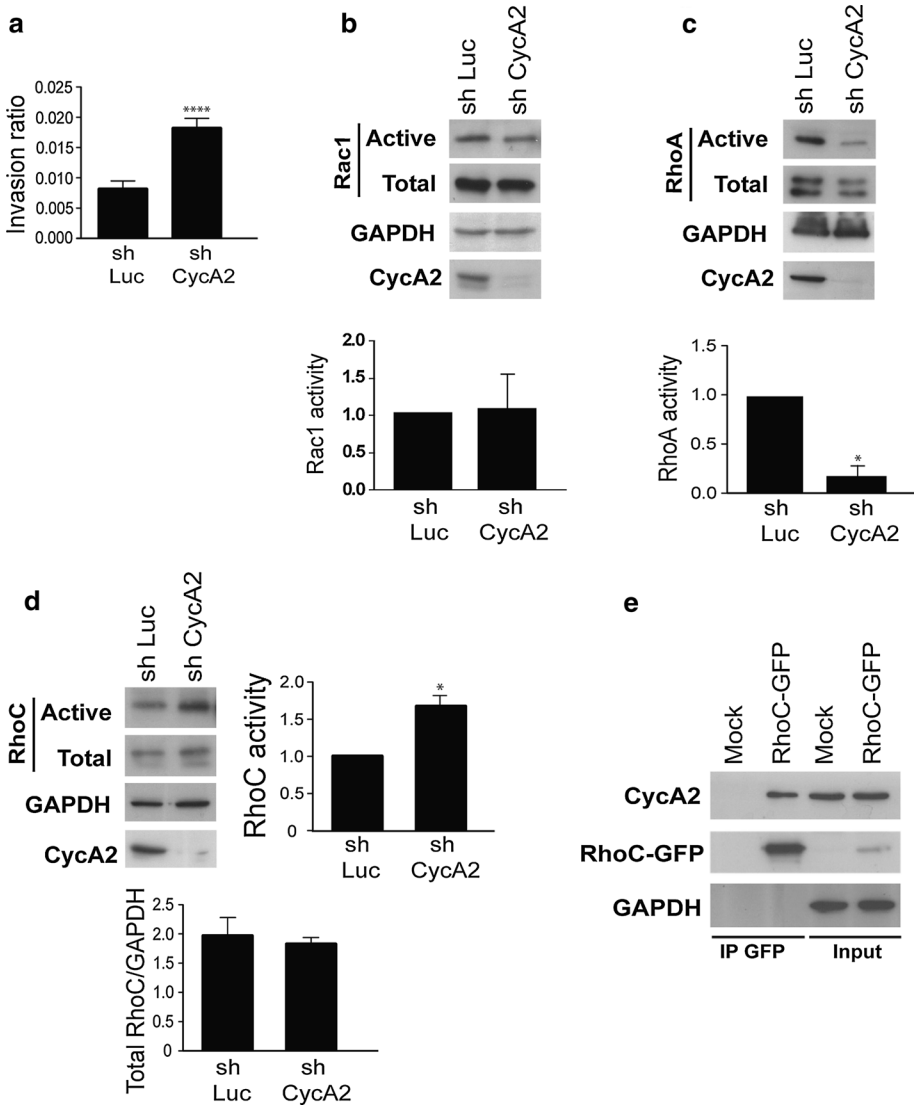

Fig. 2 Cyclin A2 knockdown in NMuMG cells modulates 3D invasion, along with RhoA and RhoC activities. **a** Invasion of sh Luc and sh CycA2 NMuMG cells in a 3D collagen matrix ($n = 5$, $^{****}P < 0.0001$). **b–d** Western blotting after pull-down of the activated forms of Rac1 (**b**), RhoA (**c**) or RhoC (**d**) in extracts of cells depleted of Cyclin A2. *Lower panels* Quantification where the amount of the GTP-bound form was normalized to total Rac1, RhoA, RhoC and GAPDH. Data are represented as mean ± SEM ($^{*}P = 0.01$ for RhoA, $n = 3$ and $^{*}P = 0.01$ for RhoC, $n = 3$). **e** Co-immunoprecipitation of endogenous Cyclin A2 with RhoC. Cell lysates obtained from NMuMG cells transfected with RhoC-GFP were incubated by GFP-Trap beads. Immunoprecipitates were subjected to SDS-PAGE and analyzed by Western blotting with an anti-Cyclin A2 antibody

their number and size (Fig. 5a). This was determined by quantification of their area and diameter, as well as by the number of viable cells recovered following their dissociation (Fig. 5b–e). This was associated with an increased resistance to anoikis in the absence of Cyclin A2 (online resource 6). Moreover, Cyclin A2-depleted cells expressed higher levels of stem cell marker mRNA, such as Nanog and Oct4 (2.5 ± 0.9, $P < 0.01$; 2.4 ± 0.9, $P < 0.01$; respectively) (Fig. 5f). Thus, Cyclin A2 depletion facilitates the promotion of stem cell-like properties.

Cyclin A2 inactivation increases extravasation and migration in vivo

Extravasation and migration of cancer cells within the stroma can be limiting steps during metastatic spread [21, 34]. We tested the extravasation potential and the ability of Cyclin A2-depleted cells to invade the stroma in vivo using an avian embryo model (Leong et al.). GFP-expressing NMuMG cells with the desired phenotype with respect to Cyclin A2 and RasV12 were injected intravenously (IV) into embryos, and the cells were followed while undergoing trans-endothelial migration within the chorioallantoic membrane. Stitched images of a region of interest (ROI) in each embryo were acquired immediately and 24 h post-injection to measure the number of cells that had extravasated. As shown in Fig. 6a, NMuMG cells depleted for Cyclin A2 showed more extravasation than control cells, even if the overall percentage remained low (4.7 ± 1.52 % for sh CycA2 NMuMG cells versus 0.76 ± 0.31 % for control cells, $n = 5$ embryos per group, >100 cells analyzed per embryo, $P = 0.0354$). In contrast, NMuMG cells expressing activated RasV12 exhibited high extravasation independently of Cyclin A2 status (28.52 ± 4.62 % in control, 33.97 ± 5.54 % in Cyclin A2-depleted cells, $n = 5$ embryos per group, >100 cells analyzed per embryo,

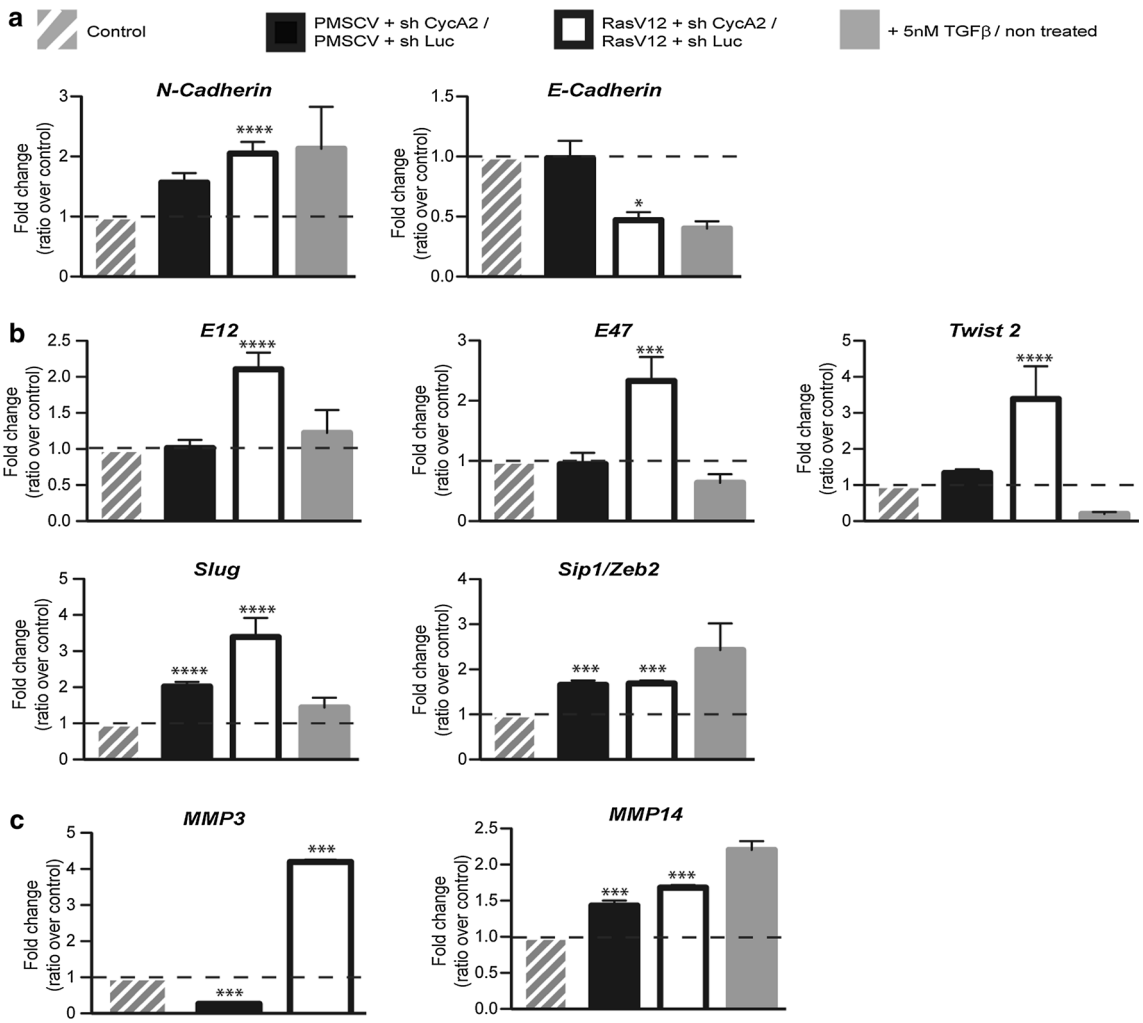

Fig. 3 Modulation of the levels of EMT markers following Cyclin A2 depletion in NMuMG RasV12 cells. mRNA analysis of EMT markers using quantitative real time PCR (qRT-PCR) and expressed as fold change, where the level in sh CycA2 cells was normalized to sh Luc cells with or without RasV12 expression. **a** mRNA levels of N-Cadherin and E-Cadherin, **b** EMT-related transcription factors and **c** metalloproteases (MMP-3 and -14)

P = ns). Next, we assessed extravascular migration of NMuMGRasV12 cells ± Cyclin A2 shRNA by performing IV injection in day 9 embryos. 3D image sets of GFP-positive micrometastatic colonies present in the stroma on day 16 of development were acquired every 15 min over a 12- to 16-h time frame (Fig. 6e). Migration of Cyclin A2-depleted cells into the stroma was enhanced, as shown by their increased average velocity (23.77 ± 1.18 μm/h for sh CycA2 cells, $n = 39$, versus 16.10 ± 0.69 μm/h for control cells, $n = 41$, $P < 0.0001$) and displacement (2.98 ± 0.25 μm/h for sh CycA2 cells, $n = 39$, versus 2.13 ± 0.25 μm/h for control cells, $n = 41$, $P = 0.0194$) (Fig. 6b, c). Further, 3D image sets of at least 5 ROI were acquired for each embryo every 15 min continuously for 12–16 h in order to generate migration tracks of individual cells within each ROI, and we observed that cells with Cyclin A2 suppression showed greatly increased motility as shown by their large migration tracks (red lines, Fig. 6d). Moreover, Cyclin A2-depleted cells displayed an obvious mesenchymal phenotype as characterized by an elongated morphology and enhanced formation of membrane protrusions (Fig. 6e and movies). Therefore, cells with Cyclin A2 inactivation retain their mesenchymal properties to enhance extravasation and, in a context of transformation, augment cell migration in vivo.

Discussion

Our results show that NMuMG cells deficient for Cyclin A2 undergo EMT. In particular, Fibronectin and N-Cadherin levels increase, while those of E-Cadherin decrease

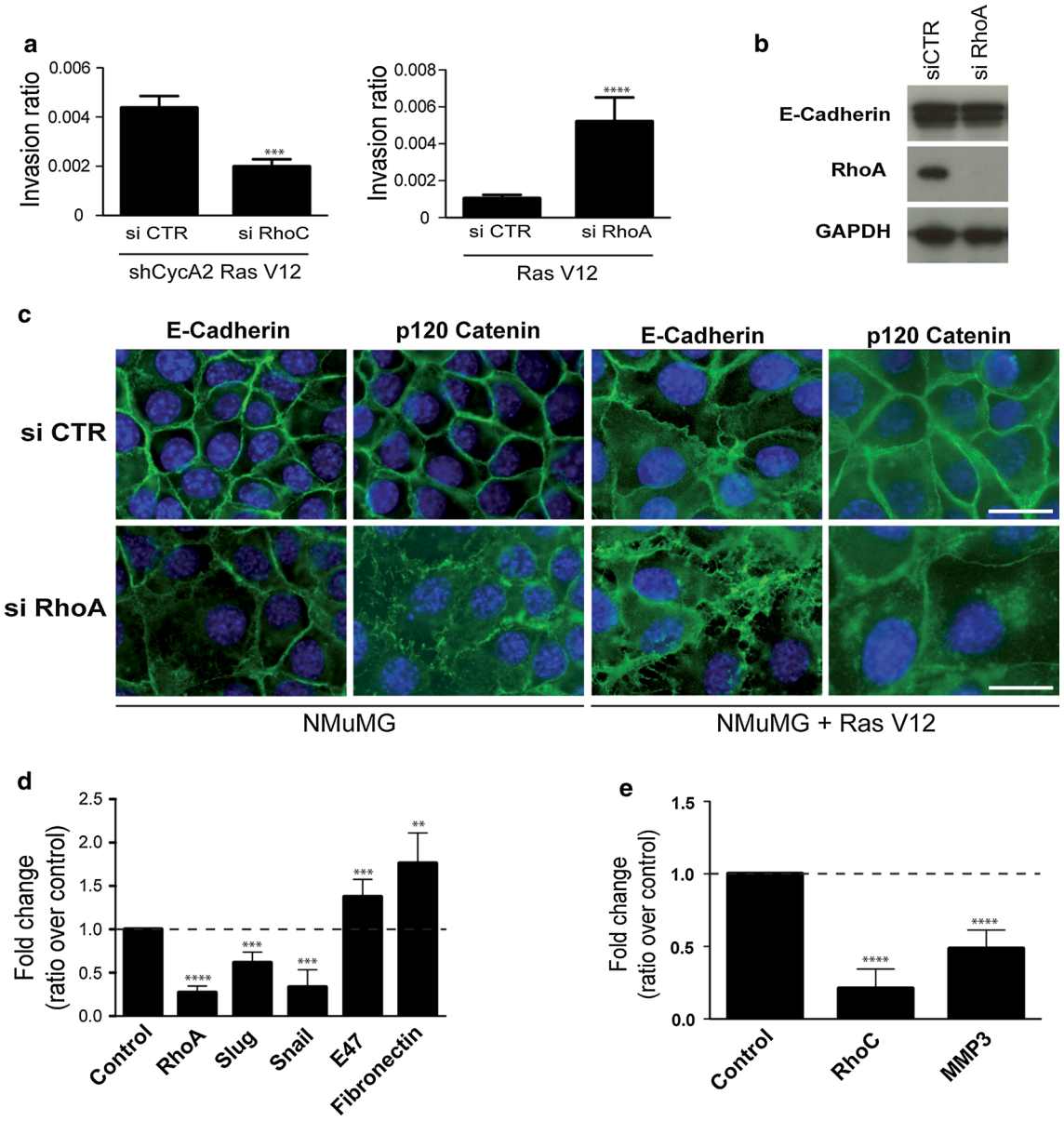

Fig. 4 Impact of RhoA and RhoC knockdown ± that of Cyclin A2 in NMuMGRasV12 cells. **a** Invasion in collagen matrix (3D) of NMuMGRasV12 cells knocked down for both RhoC and Cyclin A2 (*left panel*) or for RhoA alone (*right panel*) ($n = 3$, $^{****}P < 0.0001$ for siRhoC and $n = 3$, $^{***}P < 0.0002$ for siRhoA). **b** Western blot analysis of E-Cadherin and RhoA depletion in NMuMGRasV12 cells. **c,** Analysis of E-Cadherin and p120 Catenin cellular localization in NMuMG and NMuMGRasV12 cells treated with siRNA RhoA. qPCR analysis of mRNA levels of EMT markers in NMuMGRasV12 cells knocked-down for RhoA (**d**) or both RhoC and Cyclin A2 (**e**). Results are shown as fold change of siRNA of interest knockdowns over control knockdowns (NMuMGRasV12 cells were used for the siRhoA and sh CycA2NMuMUGRasV12 cells for siRhoC). Data are represented as mean ± SEM. $^{*}P < 0.05$, $^{**}P < 0.01$, $^{***}P < 0.001$, $^{****}P < 0.0001$

and delocalize from the plasma membrane to the cytoplasm, which corresponds to a loosening of cell–cell contacts. Transformation by RasV12 amplifies these effects on a plethora of EMT markers: upregulation of mRNA coding for N-Cadherin, the transcriptional regulators Twist2, Slug, E12 and E47, the metalloproteases MMP-3 and -14 and cancer stem cell markers including Nanog and Oct4. The invasive properties conferred by suppression of Cyclin A2 appear to be mediated in a large part by RhoA and RhoC. Accordingly, silencing of RhoA was able to recapitulate some of the phenotypes of Cyclin A2 depletion (E-Cadherin localization, increased accumulation of some mRNAs encoding EMT markers) and enhanced invasiveness [43]. Numerous studies link decreased RhoA activity to an increased invasion potential [45], and during the EMT process in development, downregulation of RhoA is crucial

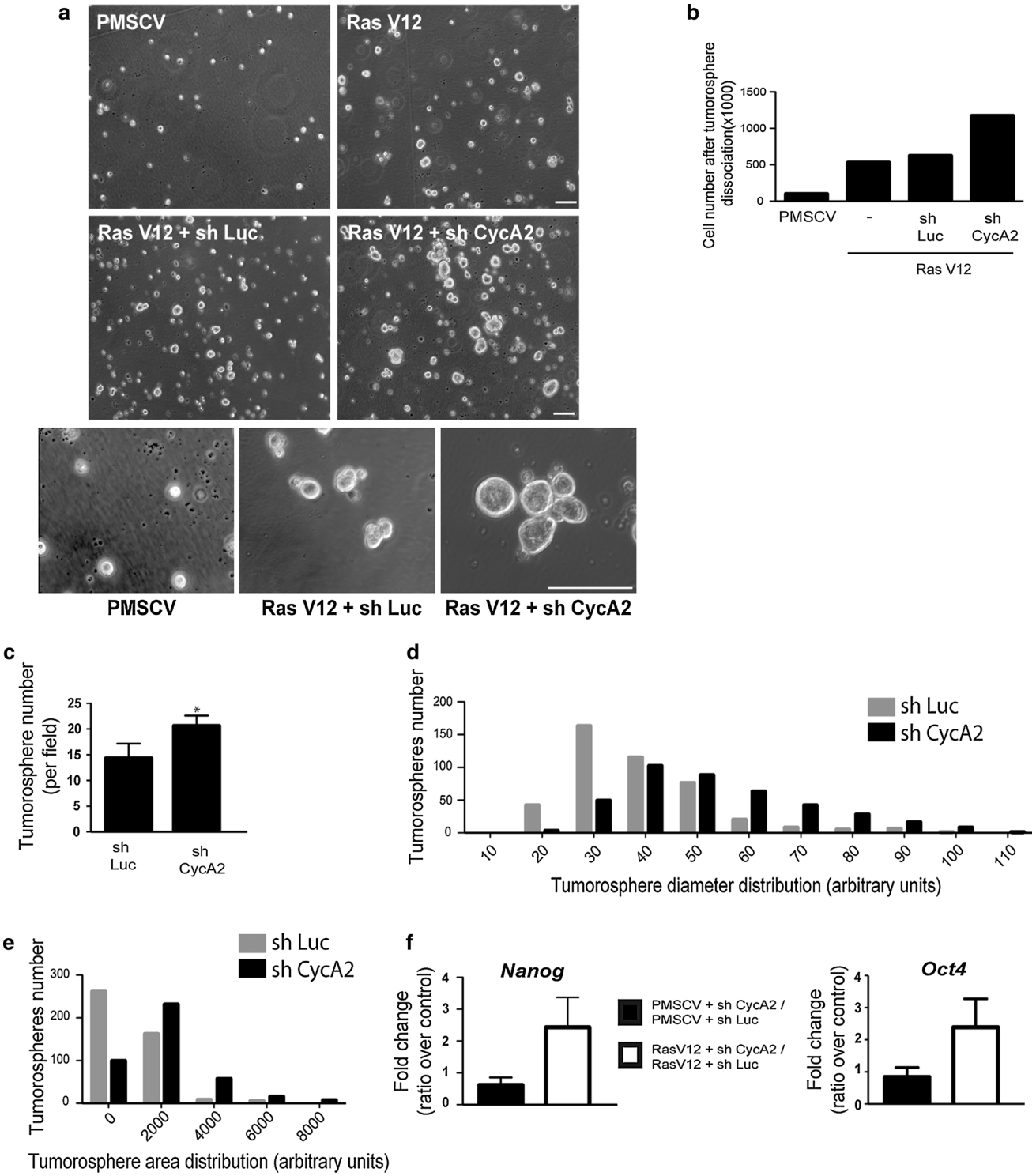

Fig. 5 Cyclin A2 knockdown enhances tumorosphere formation in NMuMGRasV12 cells. **a** Visualization of tumorosphere formation by light microscopy in sh Luc and sh CycA2 NMuMGRasV12 cells. *Scale bar* 100 μM. **b** Cell numbers after dissociation of tumorospheres formed by cells expressing RasV12 with or without Cyclin A2 knockdown ($n = 3$, $^{*}P = 0.03$). **c** Tumorosphere number, diameter (**d**) and area (**e**) represented as frequency distribution in NMuMGRasV12 Cyclin A2-depleted cells relative to cells expressing the sh Luc control ($n = 3$, $^{****}P < 0.001$). **f** mRNA levels of Nanog and Oct4 by qRT-PCR and expressed as fold change, where the level in sh CycA2 cells was normalized to sh Luc infected cells with or without RasV12 expression. Data are represented as mean ± SEM. $^{***}P < 0.001$

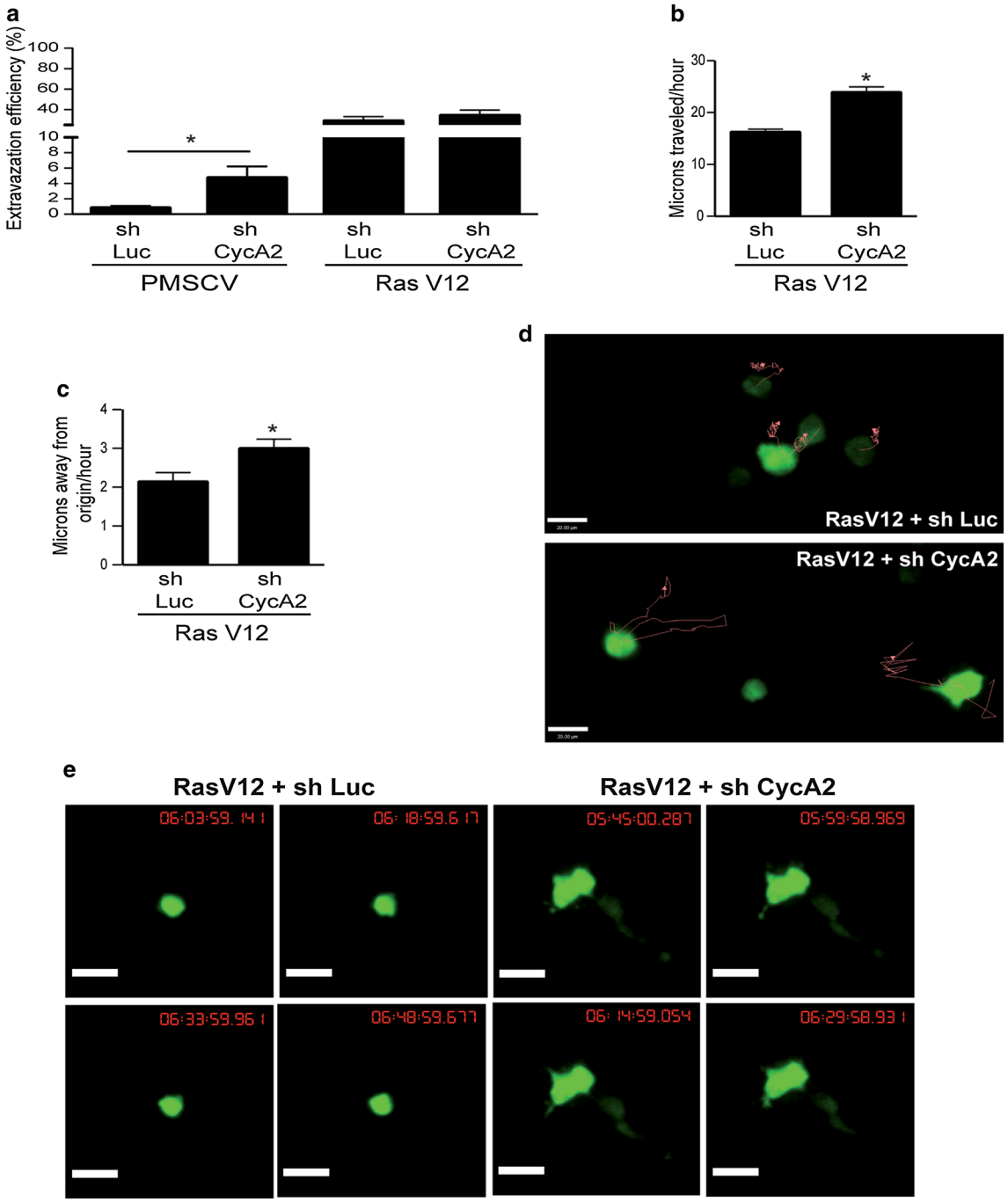

Fig. 6 Cyclin A2 knockdown modulates extravasation and migration in avian embryos. **a** Extravasation of sh Luc and sh CycA2 NMuMG cells with or without RasV12 expression. The data represent the percentage of cells present in the stroma versus the total cell number detected in the ROI. **b** Velocity of sh Luc and sh CycA2 NMuMGRasV12 cells expressed in microns traveled per hour. **c** Displacement of sh Luc and sh CycA2 NMuMGRasV12 cells expressed in microns traveled away from the origin. **d** Migration tracks (*red line*) of sh Luc and sh CycA2 NMuMGRasV12 cells within CAM stroma as analyzed by Volocity software. **e** Image set of sh Luc and sh CycA2 NMuMGRasV12 cells present in the stroma. Images were acquired every 15 min for 12–16 h. Data are represented as mean ± SEM. $^*P < 0.05$

for cytoskeletal and basement membrane reorganization in order for displacement of EMT cells to occur [31]. Cyclin A2 directly interacts with RhoA and potentiates the exchange activity of its GEFs, which is in accordance with the reduced RhoA activation we see in absence of Cyclin A2. Besides, p120 Catenin also accumulates in the

cytoplasm in Cyclin A2-depleted cells, a situation that has been shown to lead to the formation of an inhibitory p120 Catenin/RhoA complex [2]. These two observations offer the most reasonable explanation for the reduced RhoA activity observed when Cyclin A2 is ablated.

In contrast to RhoA, we found that knockdown of RhoC in Cyclin A2-depleted cells compromised mainly their invasive properties. Hakem et al. established the requirement for RhoC in the spreading of tumor cells using the metastasis-prone mouse strain *MMTV-PyMT* [18]. Further, recent studies highlighted RhoC as a major regulator of EMT-mediated invasion [6, 27], where RhoC activity was correlated to its increased expression. We detected no significant variation in RhoC level, pointing to a possible regulation of its activation via its interaction with Cyclin A2. This offers a potential mechanism for RhoC to modulate invasion during EMT. RhoA through Dia has been shown to stabilize Adherens Junctions (AJ), whereas RhoC via ROCK promotes the delocalization of AJ components such as p120 Catenin, α Catenin and β Catenin [37], the main effector of the Wnt canonical pathway that is involved in the regulation of EMT through transcriptional activity following its protein stabilization [14, 16, 33]. In two studies, Cyclin A2/CDK2 has been shown to enhance β Catenin degradation [20, 32] which could explain the increased β Catenin protein levels and nuclear localization we observed following Cyclin A2 depletion. The involvement of the β Catenin/Wnt pathway in the induction of EMT caused by Cyclin A2 depletion requires further investigation. Thus, loss of Cyclin A2 potentiates EMT and conceivably metastatic potential in part through the opposite regulation of RhoA and RhoC.

The in vivo outcomes of the phenotypes that were observed in vitro were analyzed in a classic model of metastasis, the avian embryo model. Consistent with the increased invasion we observed in vitro, we found that extravasation was enhanced in NMuMG cells inactivated for Cyclin A2 by comparison to control. Therefore, in non-transformed conditions, Cyclin A2 depletion confers motility advantage to cells in vivo, which was abolished under a more potent transformation agent such as oncogenic RasV12 expression. Of note, cells with Cyclin A2 suppression in the background of RasV12 expression harbored a mesenchymal phenotype and were highly motile during migration in the underlying stroma of avian embryos. This confirms that EMT had occurred in these cells enabling them to migrate further and faster, as demonstrated by enhanced displacement, velocity and migration tracks, as compared to control cells. It has been reported that differences in post-extravasation migration between cell types are correlated with metastatic ability [30]. Given the increased migration of Cyclin A2 depleted cells in this context, we hypothesize that they would generate higher metastases numbers. However, the potency of the cells depleted for Cyclin A2 to replicate and form tumors in the stroma remains to be established.

Another outcome of Cyclin A2 knockdown was the augmentation of the number and size of tumorospheres. This reflects a corresponding increase in resistance to anoïkis and continued proliferation in non-adherent conditions and characteristics that have previously been demonstrated to correlate with cancer stemness, and further supported by increased levels of Nanog and Oct4, markers of cancer stem cells. Several elegant studies have shown that induction of EMT, by expression of master transcription factors such as Zeb1/2, Snail or Slug, increases CSC properties including expression of cell surface markers ($CD44^{high}/CD24^{low}$ in breast CSCs), high tumor initiation capability and formation of tumorospheres [8, 12, 50]. Cancer stem cells are thought to be a small population of cancer cells that have the ability of unlimited growth, self renewal, transdifferentiation capability and high tumorigenicity upon injection into immunodeficient mice [44]. With the data from the avian embryo system, these observations have major implications on the capacity of a cell to leave the primary tumor and to generate a macroscopic secondary tumor. This correlates with the diminished level of Cyclin A2 protein in metastases versus the corresponding primary tumor [1, 4, 15, 25, 29, 46]. We believe that our observations implicating Cyclin A2 in the process of EMT help explain why low Cyclin A2 expression is associated with poor prognosis in some cancers [1, 4, 15, 25, 29, 46].

Acknowledgments This work was supported by a grant from the Association pour la Recherche contre le Cancer (ARC). N.B. was supported by fellowships from the French Ministry of Education and Research and the Fondation pour la Recherche Médicale (FRM). C.C. was supported by fellowships from the Canadian Institutes of Health Research and La Ligue Contre le Cancer. The authors declare no competing financial interests. This work was made possible thanks to the MRI imaging facility. We are grateful to Robert Hipskind, Gilles Gadéa and Pierre Roux for their helpful discussions and comments on our manuscript.

Conflict of interest The authors disclose no potential conflicts of interest.

References

1. Aaltomaa S, Lipponen P, Ala-Opas M, Eskelinen M, Syrjanen K, Kosma VM (1999) Expression of cyclins A and D and p21(waf1/cip1) proteins in renal cell cancer and their relation to clinicopathological variables and patient survival. Br J Cancer 80:2001–2007
2. Anastasiadis PZ, Moon SY, Thoreson MA, Mariner DJ, Crawford HC, Zheng Y, Reynolds AB (2000) Inhibition of RhoA by p120 catenin. Nat Cell Biol 2:637–644
3. Arpaia E, Blaser H, Quintela-Fandino M, Duncan G, Leong HS, Ablack A, Nambiar SC, Lind EF, Silvester J, Fleming CK, Rufini

A, Tusche MW, Brustle A, Ohashi PS, Lewis JD, Mak TW (2012) The interaction between caveolin-1 and Rho-GTPases promotes metastasis by controlling the expression of alpha5-integrin and the activation of Src, Ras and Erk. Oncogene 31:884–896
4. Arsic N, Bendris N, Peter M, Begon-Pescia C, Rebouissou C, Gadea G, Bouquier N, Bibeau F, Lemmers B, Blanchard JM (2012) A novel function for Cyclin A2: control of cell invasion via RhoA signaling. J Cell Biol 196:147–162
5. Barrallo-Gimeno A, Nieto MA (2005) The Snail genes as inducers of cell movement and survival: implications in development and cancer. Development 132:3151–3161
6. Bellovin DI, Simpson KJ, Danilov T, Maynard E, Rimm DL, Oettgen P, Mercurio AM (2006) Reciprocal regulation of RhoA and RhoC characterizes the EMT and identifies RhoC as a prognostic marker of colon carcinoma. Oncogene 25:6959–6967
7. Bendris N, Arsic N, Lemmers B, Blanchard JM (2012) Cyclin A2, Rho GTPases and EMT. Small Gtpases 3:225–228
8. Bhat-Nakshatri P, Appaiah H, Ballas C, Pick-Franke P, Goulet R Jr, Badve S, Srour EF, Nakshatri H (2010) SLUG/SNAI2 and tumor necrosis factor generate breast cells with CD44+/CD24- phenotype. BMC Cancer 10:411
9. Blanchard JM (2014) To be or not to be a proliferation marker? Oncogene 33:954–955
10. Borm B, Requardt RP, Herzog V, Kirfel G (2005) Membrane ruffles in cell migration: indicators of inefficient lamellipodia adhesion and compartments of actin filament reorganization. Exp Cell Res 302:83–95
11. Chapman HA (2011) Epithelial-mesenchymal interactions in pulmonary fibrosis. Annu Rev Physiol 73:413–435
12. Chu PY, Hu FW, Yu CC, Tsai LL, Yu CH, Wu BC, Chen YW, Huang PI, Lo WL (2012) Epithelial-mesenchymal transition transcription factor ZEB1/ZEB2 co-expression predicts poor prognosis and maintains tumor-initiating properties in head and neck cancer. Oral Oncol 49:34–41
13. Coisy M, Roure V, Ribot M, Philips A, Muchardt C, Blanchard JM, Dantonel JC (2004) Cyclin A repression in quiescent cells is associated with chromatin remodeling of its promoter and requires Brahma/SNF2alpha. Mol Cell 15:43–56
14. Conacci-Sorrell M, Simcha I, Ben-Yedidia T, Blechman J, Savagner P, Ben-Ze'ev A (2003) Autoregulation of E-cadherin expression by cadherin–cadherin interactions: the roles of beta-catenin signaling, Slug, and MAPK. J Cell Biol 163:847–857
15. Davidson B, Risberg B, Berner A, Nesland JM, Trope CG, Kristensen GB, Bryne M, Goscinski M, van de Putte G, Florenes VA (2001) Expression of cell cycle proteins in ovarian carcinoma cells in serous effusions-biological and prognostic implications. Gynecol Oncol 83:249–256
16. Fodde R, Smits R, Clevers H (2001) APC, signal transduction and genetic instability in colorectal cancer. Nat Rev Cancer 1:55–67
17. Guo W, Keckesova Z, Donaher JL, Shibue T, Tischler V, Reinhardt F, Itzkovitz S, Noske A, Zurrer-Hardi U, Bell G, Tam WL, Mani SA, van Oudenaarden A, Weinberg RA (2012) Slug and sox9 cooperatively determine the mammary stem cell state. Cell 148:1015–1028
18. Hakem A, Sanchez-Sweatman O, You-Ten A, Duncan G, Wakeham A, Khokha R, Mak TW (2005) RhoC is dispensable for embryogenesis and tumor initiation but essential for metastasis. Genes Dev 19:1974–1979
19. Heasman SJ, Ridley AJ (2008) Mammalian Rho GTPases: new insights into their functions from in vivo studies. Nat Rev Mol Cell Biol 9:690–701
20. Kim SI, Park CS, Lee MS, Kwon MS, Jho EH, Song WK (2004) Cyclin-dependent kinase 2 regulates the interaction of Axin with beta-catenin. Biochem Biophys Res Commun 317:478–483
21. Koop S, Schmidt EE, MacDonald IC, Morris VL, Khokha R, Grattan M, Leone J, Chambers AF, Groom AC (1996) Independence of metastatic ability and extravasation: metastatic ras-transformed and control fibroblasts extravasate equally well. Proc Natl Acad Sci U S A 93:11080–11084
22. Larue L, Bellacosa A (2005) Epithelial-mesenchymal transition in development and cancer: role of phosphatidylinositol 3′ kinase/AKT pathways. Oncogene 24:7443–7454
23. Leong HS, Lizardo MM, Ablack A, McPherson VA, Wandless TJ, Chambers AF, Lewis JD (2012) Imaging the impact of chemically inducible proteins on cellular dynamics in vivo. PLoS One 7:e30177
24. Leong HS, Steinmetz NF, Ablack A, Destito G, Zijlstra A, Stuhlmann H, Manchester M, Lewis JD (2010) Intravital imaging of embryonic and tumor neovasculature using viral nanoparticles. Nat Protoc 5:1406–1417
25. Li JQ, Miki H, Wu F, Saoo K, Nishioka M, Ohmori M, Imaida K (2002) Cyclin A correlates with carcinogenesis and metastasis, and p27(kip1) correlates with lymphatic invasion, in colorectal neoplasms. Hum Pathol 33:1006–1015
26. Lo HW, Hsu SC, Xia W, Cao X, Shih JY, Wei Y, Abbruzzese JL, Hortobagyi GN, Hung MC (2007) Epidermal growth factor receptor cooperates with signal transducer and activator of transcription 3 to induce epithelial-mesenchymal transition in cancer cells via up-regulation of TWIST gene expression. Cancer Res 67:9066–9076
27. Ma L, Teruya-Feldstein J, Weinberg RA (2007) Tumour invasion and metastasis initiated by microRNA-10b in breast cancer. Nature 449:682–688
28. Mani SA, Guo W, Liao MJ, Eaton EN, Ayyanan A, Zhou AY, Brooks M, Reinhard F, Zhang CC, Shipitsin M, Campbell LL, Polyak K, Brisken C, Yang J, Weinberg RA (2008) The epithelial-mesenchymal transition generates cells with properties of stem cells. Cell 133:704–715
29. Mashal RD, Lester S, Corless C, Richie JP, Chandra R, Propert KJ, Dutta A (1996) Expression of cell cycle-regulated proteins in prostate cancer. Cancer Res 56:4159–4163
30. Morris VL, Koop S, MacDonald IC, Schmidt EE, Grattan M, Percy D, Chambers AF, Groom AC (1994) Mammary carcinoma cell lines of high and low metastatic potential differ not in extravasation but in subsequent migration and growth. Clin Exp Metastasis 12:357–367
31. Nakaya Y, Sukowati EW, Wu Y, Sheng G (2008) RhoA and microtubule dynamics control cell-basement membrane interaction in EMT during gastrulation. Nat Cell Biol 10:765–775
32. Park CS, Kim SI, Lee MS, Youn CY, Kim DJ, Jho EH, Song WK (2004) Modulation of beta-catenin phosphorylation/degradation by cyclin-dependent kinase 2. J Biol Chem 279:19592–19599
33. Peifer M, Polakis P (2000) Wnt signaling in oncogenesis and embryogenesis–a look outside the nucleus. Science 287:1606–1609
34. Philippar U, Roussos ET, Oser M, Yamaguchi H, Kim HD, Giampieri S, Wang Y, Goswami S, Wyckoff JB, Lauffenburger DA, Sahai E, Condeelis JS, Gertler FB (2008) A Mena invasion isoform potentiates EGF-induced carcinoma cell invasion and metastasis. Dev Cell 15:813–828
35. Ru GQ, Wang HJ, Xu WJ, Zhao ZS (2011) Upregulation of twist in gastric carcinoma associated with tumor invasion and poor prognosis. Pathol Oncol Res 17:341–347
36. Sahai E, Marshall CJ (2002) RHO-GTPases and cancer. Nat Rev Cancer 2:133–142
37. Sahai E, Marshall CJ (2002) ROCK and Dia have opposing effects on adherens junctions downstream of Rho. Nat Cell Biol 4:408–415
38. Smith HW, Marra P, Marshall CJ (2008) uPAR promotes formation of the p130Cas-Crk complex to activate Rac through DOCK180. J Cell Biol 182:777–790
39. Sobrado VR, Moreno-Bueno G, Cubillo E, Holt LJ, Nieto MA, Portillo F, Cano A (2009) The class I bHLH factors E2-2A and E2-2B regulate EMT. J Cell Sci 122:1014–1024

40. Thiery JP (2002) Epithelial-mesenchymal transitions in tumour progression. Nat Rev Cancer 2:442–454
41. Thiery JP, Acloque H, Huang RY, Nieto MA (2009) Epithelial-mesenchymal transitions in development and disease. Cell 139:871–890
42. Thiery JP, Sleeman JP (2006) Complex networks orchestrate epithelial-mesenchymal transitions. Nat Rev Mol Cell Biol 7:131–142
43. Vega FM, Fruhwirth G, Ng T, Ridley AJ (2011) RhoA and RhoC have distinct roles in migration and invasion by acting through different targets. J Cell Biol 193:655–665
44. Vermeulen L, de Sousa e Melo F, Richel DJ, Medema JP (2012) The developing cancer stem-cell model: clinical challenges and opportunities. Lancet Oncol 13:e83–e89
45. Wang W, Wu F, Fang F, Tao Y, Yang L (2008) Inhibition of invasion and metastasis of hepatocellular carcinoma cells via targeting RhoC in vitro and in vivo. Clin Cancer Res 14:6804–6812
46. Wang YF, Chen JY, Chang SY, Chiu JH, Li WY, Chu PY, Tai SK, Wang LS (2008) Nm23-H1 expression of metastatic tumors in the lymph nodes is a prognostic indicator of oral squamous cell carcinoma. Int J Cancer 122:377–386
47. Yang J, Mani SA, Donaher JL, Ramaswamy S, Itzykson RA, Come C, Savagner P, Gitelman I, Richardson A, Weinberg RA (2004) Twist, a master regulator of morphogenesis, plays an essential role in tumor metastasis. Cell 117:927–939
48. Yang MH, Hsu DS, Wang HW, Wang HJ, Lan HY, Yang WH, Huang CH, Kao SY, Tzeng CH, Tai SK, Chang SY, Lee OK, Wu KJ (2010) Bmi1 is essential in Twist1-induced epithelial-mesenchymal transition. Nat Cell Biol 12:982–992
49. Zavadil J, Bottinger EP (2005) TGF-beta and epithelial-to-mesenchymal transitions. Oncogene 24:5764–5774
50. Zhu LF, Hu Y, Yang CC, Xu XH, Ning TY, Wang ZL, Ye JH, Liu LK (2012) Snail overexpression induces an epithelial to mesenchymal transition and cancer stem cell-like properties in SCC9 cells. Lab Invest 92:744–752